

5-4-2016

# The Evolution of the Surface of the Mineral Schreibersite in Prebiotic Chemistry

Nikita L. La Cruz  
*University of South Florida*

Danna Qasim  
*Kennesaw State University*

Heather Abbott-Lyon  
*Kennesaw State University, habbott@kennesaw.edu*

Claire Pirim  
*Université Lille 1*

Follow this and additional works at: <https://digitalcommons.kennesaw.edu/facpubs>

 Part of the [Biochemistry Commons](#), and the [Chemistry Commons](#)

---

## Recommended Citation

La Cruz, Nikita L.; Qasim, Danna; Abbott-Lyon, Heather; and Pirim, Claire, "The Evolution of the Surface of the Mineral Schreibersite in Prebiotic Chemistry" (2016). *Faculty Publications*. 3748.  
<https://digitalcommons.kennesaw.edu/facpubs/3748>

This Article is brought to you for free and open access by DigitalCommons@Kennesaw State University. It has been accepted for inclusion in Faculty Publications by an authorized administrator of DigitalCommons@Kennesaw State University. For more information, please contact [digitalcommons@kennesaw.edu](mailto:digitalcommons@kennesaw.edu).



Cite this: *Phys. Chem. Chem. Phys.*,  
2016, **18**, 20160

## The evolution of the surface of the mineral schreibersite in prebiotic chemistry

Nikita L. La Cruz,<sup>a</sup> Danna Qasim,<sup>b</sup> Heather Abbott-Lyon,<sup>b</sup> Claire Pirim,<sup>c</sup>  
Aaron D. McKee,<sup>d</sup> Thomas Orlando,<sup>d</sup> Maheen Gull,<sup>a</sup> Danny Lindsay<sup>a</sup> and  
Matthew A. Pasek<sup>\*a</sup>

We present a study of the reactions of the meteoritic mineral schreibersite (Fe,Ni)<sub>3</sub>P, focusing primarily on surface chemistry and prebiotic phosphorylation. In this work, a synthetic analogue of the mineral was synthesized by mixing stoichiometric proportions of elemental iron, nickel and phosphorus and heating in a tube furnace at 820 °C for approximately 235 hours under argon or under vacuum, a modification of the method of Skála and Drábek (2002). Once synthesized, the schreibersite was characterized to confirm the identity of the product as well as to elucidate the oxidation processes affecting the surface. In addition to characterization of the solid product, this schreibersite was reacted with water or with organic solutes in a choline chloride–urea deep eutectic mixture, to constrain potential prebiotic products. Major inorganic solutes produced by reaction of water include orthophosphate, phosphite, pyrophosphate and hypophosphate consistent with prior work on Fe<sub>3</sub>P corrosion. Additionally, schreibersite corrodes in water and dries down to form a deep eutectic solution, generating phosphorylated products, in this case phosphocholine, using this synthesized schreibersite.

Received 5th February 2016,  
Accepted 3rd May 2016

DOI: 10.1039/c6cp00836d

www.rsc.org/pccp

### 1. Introduction

Phosphorus is an important element in modern biochemistry as it is present in biomolecules such as phospholipids (cellular structure), DNA and RNA (storage and transfer of genetic information), and ATP and coenzymes (energetics).<sup>1</sup> Although phosphorus is ubiquitous in biological systems, it is poorly reactive towards organic molecules, and hence the facile synthesis of prebiotic phosphorus compounds using terrestrial phosphate minerals has been hindered by the low reactivity and solubility of phosphates such as apatite.<sup>2</sup> Several researchers have attempted to overcome this difficulty by adding reactive organics as condensing agents to promote a dehydration reaction,<sup>3</sup> or have added heat to promote drying down of the organic–phosphate mix to make organophosphates.<sup>4</sup> Still other researchers have used condensed phosphates (adding chemical energy to the phosphate instead of the organic),<sup>5</sup> or have used solvents other than water such as formamide to promote the dehydration reaction.<sup>6,7</sup> Many of

these routes have been questioned by other chemists as using implausible reactants or unlikely starting phosphate sources.<sup>8,9</sup>

How then were the P–O–C bonds that are so ubiquitous in biochemistry made, starting with a prebiotically plausible mineral source? Pasek and Lauretta (2005) and Bryant and Kee (2006) together presented a hypothesis that meteoritic mineral schreibersite—formula (Fe,Ni)<sub>3</sub>P—could have been the source of reactive P for the development of prebiotic phosphorylated biomolecules.<sup>10,11</sup> This was based on the formation of phosphite and other soluble P compounds when schreibersite reacts with water, coupled with the arguments made by Gulick (1955) for reduced P species being more prebiotically available.<sup>12</sup>

Phosphide minerals such as schreibersite contain phosphorus (P) in a reduced oxidation state as opposed to the oxidized P<sup>5+</sup> containing minerals that are ubiquitous on the earth. The oxidation state of the P in schreibersite is approximately –1 based on binding energies obtained from X-ray photoelectron spectroscopy (XPS) studies.<sup>13–15</sup> This is effectively equivalent to phosphorus forming a metallic alloy with Fe and Ni. Since most environments on the earth have an oxidizing character, phosphide minerals are rarely found on the earth. Notable exceptions are the phosphides recently discovered near the Dead Sea and iron phosphide in fulgurites.<sup>16–18</sup> Together, these minerals probably account for very little of the total surficial P on the earth, thus meteoritic sources are likely more important for providing phosphide minerals to geologic environments.

Meteoritic sources of P may have been an important source due to their high reactivity and high flux on the early earth.<sup>19</sup>

<sup>a</sup> School of Geosciences, University of South Florida, NES 204, 4202 E Fowler Ave, Tampa, FL 33620, USA. E-mail: mpasek@usf.edu; Tel: +813-974-8979

<sup>b</sup> Department of Chemistry and Biochemistry, Kennesaw State University, Kennesaw, GA 30144, USA

<sup>c</sup> Laboratoire de Physique des Lasers, Atomes et Molécules (PhLAM), UMR 8523 CNRS, Université Lille 1, 59655 Villeneuve d'Ascq, France

<sup>d</sup> School of Chemistry and Biochemistry, Georgia Institute of Technology, Atlanta, GA 30332, USA

Evidence from the terrestrial geologic record and models of the accretion of extraterrestrial material to the early earth suggest the flux of material to the early earth was high enough to have added a few percent to the mass of the earth 4.4 billion years ago.<sup>20</sup> The timing of the quiescence of this bombardment roughly corresponds to the best guesses for the origination time of life. To this end, meteoritic material played a potentially important role in the origin and development of life on the earth. As an example of the role meteorites might have played in the delivery of phosphorus, Pasek *et al.* (2013) demonstrated that some of the earliest carbonate rocks appear to bear small quantities of phosphite, suggesting a meteoritic P component to the early earth's oceans, or at the least, suggesting that the oxidation state of nutrients in the earth's ocean was different early in earth's history.<sup>21</sup>

### 1.1 Schreibersite oxidation pathway

It is unclear from prior phosphorylation experiments involving phosphide minerals where the phosphorylation reaction takes place: in solution or on the schreibersite surface.<sup>15,22</sup> Solutional chemistry would require a reactive solute to phosphorylate an organic. Such a solute might be trimetaphosphate,<sup>5</sup> which can be synthesized from schreibersite albeit in very small concentrations *via* oxidation.<sup>23</sup> However, the yields of phosphorylated product exceed the amount of trimetaphosphate produced, suggesting an alternative pathway.

It is plausible that the surface of the schreibersite is the reactive site for phosphorylation in these experiments. However, in order for the surface to be involved in these reactions, there must be a layer of oxidized material present to generate the phosphate that is subsequently incorporated into the phosphorylated molecules. Prior works examining the surface of natural schreibersite minerals have demonstrated a thin coating of oxides/phosphates consistent with an oxidized surface.<sup>14,15,24</sup> However, these analyses were performed on samples that had been exposed to the atmosphere for several years, and hence, likely reacted with atmospheric O<sub>2</sub> to produce the oxide coating. Based on the presence of detrital reduced minerals (minerals that would not have survived on the earth's surface after atmospheric oxygenation) and ferrous iron in rocks on the early earth,<sup>25</sup> the atmospheric concentration of O<sub>2</sub> was low prior to the oxygenation of the atmosphere.<sup>26</sup> Hence the surface of schreibersite may not have been oxidized by O<sub>2</sub> on the prebiotic earth. Could the surface have been oxidized by other materials, and if not, would it still be amenable to phosphorylation?

Here we present the synthesis, characterization and corrosion of artificial schreibersite. The synthesis was accomplished by modifying the method presented by Skála and Drábek (2002) and the synthesized product was characterized using petrographic as well as surface chemistry techniques to determine the efficiency of schreibersite as a reactant.<sup>27</sup> These synthesized samples were then used in experiments seeking to understand the extent of phosphorylation capable of occurring on the earth's surface by this mineral.

## 2. Methods

### 2.1 Materials

Iron (Fe) powder (98+% purity), nickel (Ni) powder (99.9% metals basis), phosphorus (P) powder (red amorphous, 98.9% metals basis), sodium hydroxide (NaOH) pellets (98%), Fe<sub>3</sub>P, and phosphorous acid (98% purity) were acquired from Alfa Aesar. Doubly deionized water was generated in house using a Barnstead (Dubuque, IA) Nanopure<sup>®</sup> Diamond analytical combined reverse osmosis-deionization system. Seawater solutions were made using an aquarium sea salt mixture produced by Instant Ocean<sup>®</sup>. Sulfidic water solutions were made using sodium sulfide (98%) obtained from EMD Chemicals. Ethylenediaminetetraacetic acid (EDTA) powder (99.4%), was obtained from Sigma Aldrich. The isopropyl alcohol (laboratory grade) used to clean samples after cutting and the hydrochloric acid (12.0 N) were obtained from Fisher Scientific. Deuterium oxide used (99.8%) was obtained from ACROS.

### 2.2 Schreibersite synthesis

Synthetic schreibersite was made using a modified version of the method outlined by Skála and Drábek in 2002.<sup>27</sup> The Fe, Ni and P powders were weighed using an Ohaus Precision advanced balance so that the molar ratio of the elements was 2 : 1 : 1. The powders were then thoroughly mixed in a mortar with a pestle and then transferred to a ceramic boat. The boat was then placed in a ThermoScientific Lindberg/Blue M 1200 °C split hinge tube furnace. At least three purges were done using argon gas and a vacuum pump. When an argon atmosphere was established in the tube, the temperature was raised to 820 °C and this temperature was maintained for approximately 235 hours.

Vesicular 'bread loaf' type samples of schreibersite were obtained by heating the sample to 820 °C and cooling rapidly (the temperature dropped from 820 °C to 25 °C in approximately a half hour by turning the furnace off and moving the ceramic boat out of the furnace along the tube using an internal hook) or slowly (temperature dropped from 820 °C to 25 °C in approximately 1 day). Dense schreibersite beads were obtained by raising the furnace temperature to 1048 °C (the eutectic melting point of schreibersite), maintaining that temperature for approximately 1 hour and then reducing the temperature to room temperature slowly. In all cases, the product obtained was weighed and the yield was determined.

### 2.3 Material and surface analyses

**X-ray diffractometry (XRD).** XRD measurements were made using an Olympus BTX Benchtop XRD system using a cobalt X-ray target material. Each sample ("bread loaf" variety) was crushed and sieved using a 150 micrometer (μm) mesh and about 20 milligrams (mg) were placed in the apparatus and XRD diffractograms were obtained.

**Electron microprobe point analysis (EMPA).** EMPA analyses were done remotely at Florida International University's (FIU) EMPA facility. The instrument used was an Electron Probe MicroAnalyzer JXA-8900-R. An accelerating voltage of 20 kV and a tube current of 20 nA were used. Pieces of each sample

(“bread loaf” and “dense” variety) were mounted in epoxy and polished prior to analysis at FIU. The percentage of Fe, Ni, and P in each sample were determined using metal standards and these values were used to determine empirical formulas of the samples.<sup>18</sup>

**X-ray photoelectron spectroscopy (XPS).** XPS data were obtained using a Thermo Scientific K-Alpha analytical XPS system and the vacuum pressure during the experiments was maintained at approximately  $7 \times 10^{-8}$  Torr. The spot size of the X-ray source was set to 400  $\mu\text{m}$  and the beam provided radiation with an energy of 1486.7 eV. Samples of crushed uncorroded and corroded “bread loaf” variety schreibersite samples were introduced into an XPS system in copper mounts, whereas dense samples of schreibersite were mounted using carbon tape so that XPS surveys and high resolution scans of the pristine and cut surfaces could be carried out. The spectra were collected after etching with  $\text{Ar}^+$  for 10 seconds to a depth of approximately 3.0 nm using a voltage of 3000 V.

## 2.4 Surface reactions

Solid samples suitable for surface analysis were prepared by pressing the crushed and sieved “dense” synthetic schreibersite into an iron plate (Alfa Aesar, 2 mm thick iron foil, 99.995% pure) using a 20 ton hydraulic press. The pressed samples were sintered under an inert argon atmosphere for 1 hour at 950 °C to form a robust solid and then polished to a mirror finish (*i.e.*, defect size < 1  $\mu\text{m}$ ) using a grinder-polisher (Buehler, Ecomet 300). Subsequently, the samples were sonicated in isopropanol and methanol before SEM-EDX analysis to confirm surface morphology and elemental composition. In vacuum, the sample was cleaned by annealing to 680 K and irradiating with electrons. Verification of a clean surface was checked by reflection absorption infrared spectroscopy (RAIRS) and temperature programmed desorption (TPD) before dosing.

Surface measurements were performed in an ultrahigh vacuum chamber with a base pressure  $< 1 \times 10^{-9}$  Torr. RAIRS spectra were obtained at a grazing incidence angle (approximately 80° to surface normal) and TPD spectra were collected using a ramp rate of 0.2 K  $\text{s}^{-1}$ . The sample temperature was controlled by cooling with liquid  $\text{N}_2$  and resistively heating the sample. Room temperature water vapor was dosed onto the surface using a variable leak valve. A detailed description of the experimental apparatus and procedures will be provided elsewhere (Qasim and Abbott-Lyon, in prep.).

## 2.5 Reactions in water and phosphorylation experiments

Corrosion experiments were done under oxic (in the presence of oxygen) and anoxic conditions (in the absence of oxygen). For the reactions done under oxic conditions, the samples were heated to approximately 40 °C and stirred in a flask containing about 25 mL of either: deionized water, deionized water with  $\text{Na}_2\text{EDTA}$ , seawater, or a sulfidic water solution (made by acidifying a 0.1 M sodium sulfide solution with hydrochloric acid) in air. The experiments done under anoxic conditions were done in a glove box in an argon atmosphere. These reactions were allowed to stir for approximately one week. After this time,

the pieces of schreibersite were analyzed using XPS and the reaction solutions were retained to be analyzed *via* P-31 NMR. The samples were analyzed using XPS utilizing the guidelines outlined previously.  $\text{Fe}_3\text{P}$ , as an analogue of schreibersite, was also analyzed before and after corrosion to determine the nature of surficial corrosion on this material.

**P-31 NMR analysis.** The supernatant from the reaction vessels was decanted into a flask and the pH of solution was adjusted to 10 using an NaOH solution. The solutions were then filtered using Whatmann no. 5 filter paper and about 10 mL of each solution were placed in a watch glass and left to evaporate to dryness. The residues were then rehydrated using approximately 0.5 mL deuterium oxide. The solutions were then filtered using inline 0.45  $\mu\text{m}$  Puradisc filters and they were transferred to NMR tubes. P-31 NMR analyses with hydrogen both coupled and decoupled to phosphorus were done for each sample using a Unity INOVA 400 spectrometer equipped with a Varian 5 mm autoswitchable probe.

**Phosphorylation of choline by synthetic schreibersite.** Approximately 5 g of  $\text{Fe}_2\text{NiP}$  (“bread loaf” variety) were added to 15 mL DI water and this mixture was constantly stirred and heated at 85–90 °C in a tightly sealed glass tube. The reaction mixture was allowed to corrode for 1 month and afterwards, the glass tube was opened and 2 g choline chloride and 1 g urea were added to the reaction mixture (following the deep eutectic phosphorylation experiments of Gull *et al.* 2014).<sup>28</sup> The reaction vessel was then sealed, stirred and heated at the same temperature for another 2 weeks. The reaction mixture was then treated with a 1 M  $\text{Na}_2\text{S}$  solution to raise the pH to a value of 11 to 12. The mixture was then filtered and prepared for NMR using the previously outlined technique.

## 3. Results

### 3.1 Synthesis

The samples synthesized had a metallic luster and were attracted to magnet. The appearance of the sample varied depending on cooling rate and peak temperature (Fig. 1). Samples that were cooled rapidly had a more glassy texture than those cooled more slowly, though the difference between porosity was primarily due to peak temperature (dense samples were made at 1048 °C, porous samples were made at 820 °C). Samples synthesized by heated to the melting point after 235 hours were dense beads; they were smooth on one side and had needle-like crystal habit on the other side. This crystal habit was not observed in the other samples that did not have clear macroscale crystals on their surface. The dense variety produced smooth surfaces when cut, whereas the “bread loaf” variety was more vesicular with jagged edges. The products were synthesized with yields above 90% in all instances. Loss of mass was probably due to volatilization of red P. After the experiments, a yellow film coated the interior of the quartz tube, possibly from the buildup of P-bearing material.

### 3.2 Characterization

**EMPA.** The empirical formulas obtained from the EMPA analyses were on average,  $\text{Fe}_{2.02}\text{Ni}_{0.96}\text{P}_{1.04}$  (number of points



**Fig. 1** Synthesized schreibersite samples. (A) Vesicular schreibersite obtained by rapid cooling. (B) Schreibersite sample obtained by slow cooling. (C) Dense schreibersite samples obtained when specimen were heated to the eutectic melting point after 235 h. Samples are 1 cm in width, defined by the width of the alumina crucible.

collected = 69) and thus confirmed that a composition equivalent to schreibersite was synthesized.

**XRD.** X-ray diffractograms of the synthesized material are provided as Fig. 2. The  $d$  values from the samples were similar to those in the literature for schreibersite (red lines beneath peaks), and therefore indicate the products had the same crystal structure as the meteoritic mineral.

**XPS.** XPS spectra of uncorroded, synthetic  $\text{Fe}_2\text{NiP}$  agree with those obtained for natural samples by Pirim *et al.* (2014).<sup>15</sup> They all contained a peak indicating the presence of a carbon impurity or adventitious carbon at  $\sim 286$  eV, also similar to natural schreibersite. The binding energy for the phosphorus 2p electron was measured to be approximately 129.7 eV (Fig. 3a), consistent with a reduced oxidation state on P, like meteoritic schreibersite.<sup>15</sup> The peak at 132–134 eV was also observed in

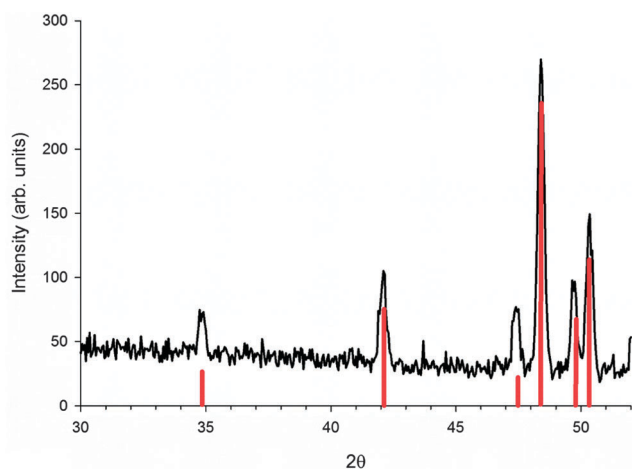


**Fig. 2** X-ray diffractogram of synthesized schreibersite (black) with comparison of characteristic  $d$  values for schreibersite (red lines).

synthetic iron phosphide,<sup>14</sup> and meteoritic schreibersite,<sup>15</sup> where it was attributed to a thin layer of oxide formed by reaction with air. The binding energies of Ni and Fe (852 eV and 706.6 eV, respectively) shows these materials remain in their elemental state. This suggests metallic bonding throughout the uncorroded material. Uncorroded iron phosphide ( $\text{Fe}_3\text{P}$ ) has a similar XPS spectrum to  $\text{Fe}_2\text{NiP}$  (Fig. 3c).

Corrosion in water results in significant changes to P binding energy. The spectra of the corroded samples indicate the presence of oxidized P on the surface of  $\text{Fe}_3\text{P}$  and  $\text{Fe}_2\text{NiP}$  (Fig. 3b & d). The dominant pre-corrosion P 2p peak (Fig. 3a & c) at 129.7 eV indicates the presence of phosphorus in the reduced phosphide state and does not shift post-corrosion in de-ionized water (Fig. 3d). The high binding energy components in panel a and c are not constrained to the primary phosphide peak by full width half maximum (FWHM) and therefore do not physically represent a single chemical environment, rather a variety of possible oxidized states of phosphorus not strongly present before corrosion. When subjected to corrosion in de-ionized water, the phosphide peak is still present, but a second peak indicative of higher oxidation state is also present (Fig. 3d). In contrast, when subjected to saltwater corrosion (Fig. 3b) the phosphide peak vanishes. A new high binding energy peak appears at 133.2 eV, suggesting the conversion of phosphorus sites previously in a reduced state to a more oxidized state, clear evidence of redox chemistry at the mineral surface. While the exact surface oxidation product is unable to be identified by XPS alone, the new peak maximum is not far from the peak maxima of  $\text{KH}_2\text{PO}_2 \times \text{H}_2\text{O}$  (line i), and  $\text{KH}_2\text{PO}_4$  (line ii). From Pelavin *et al.* (1970) these compounds represent nearly the full range of phosphorus oxyacids, +1 for hypophosphite and +5 for monobasic potassium phosphate, for plausible phosphorylating species considered in this paper.<sup>13</sup> The oxidation product, high binding peak panel b, falls between lines i and ii, suggesting an intermediately oxidized surface species. The P 2s spectra also support the evidence of phosphorus oxidation with the appearance of a higher binding energy peak post-corrosion in a similar manner as the P 2p transitions.

### 3.3 Surface reactions

RAIRS spectra of the synthetic schreibersite surface before (black spectrum) and after (blue and red spectra) exposure to  $\text{H}_2\text{O}$  are shown in Fig. 4. Water was dosed while the surface temperature ( $T_{\text{Dosed}}$ ) was held at 130 K (blue spectrum) and 295 K (red spectrum). All RAIRS spectra were collected at a surface temperature of 130 K or lower to produce a steady baseline. For the  $T_{\text{Dosed}} = 130$  K (blue spectrum), the shoulder at  $3300\text{ cm}^{-1}$  suggests the formation of amorphous water ice on the surface.<sup>29</sup> Additionally, the formation of molecular water adsorption in the form of amorphous ice is supported by the peak at  $890\text{ cm}^{-1}$ , which is representative of the libration mode of water.<sup>30–32</sup> The low pressure (*i.e.*,  $p < 10^{-8}$  Torr) and temperature (*i.e.*,  $T_{\text{Dosed}} = 130$  K) of this experiment is below the sublimation point of water. Under these conditions, it is expected that water will deposit onto any surface with a sticking coefficient of unity. The peak at  $1224\text{ cm}^{-1}$  is in good agreement

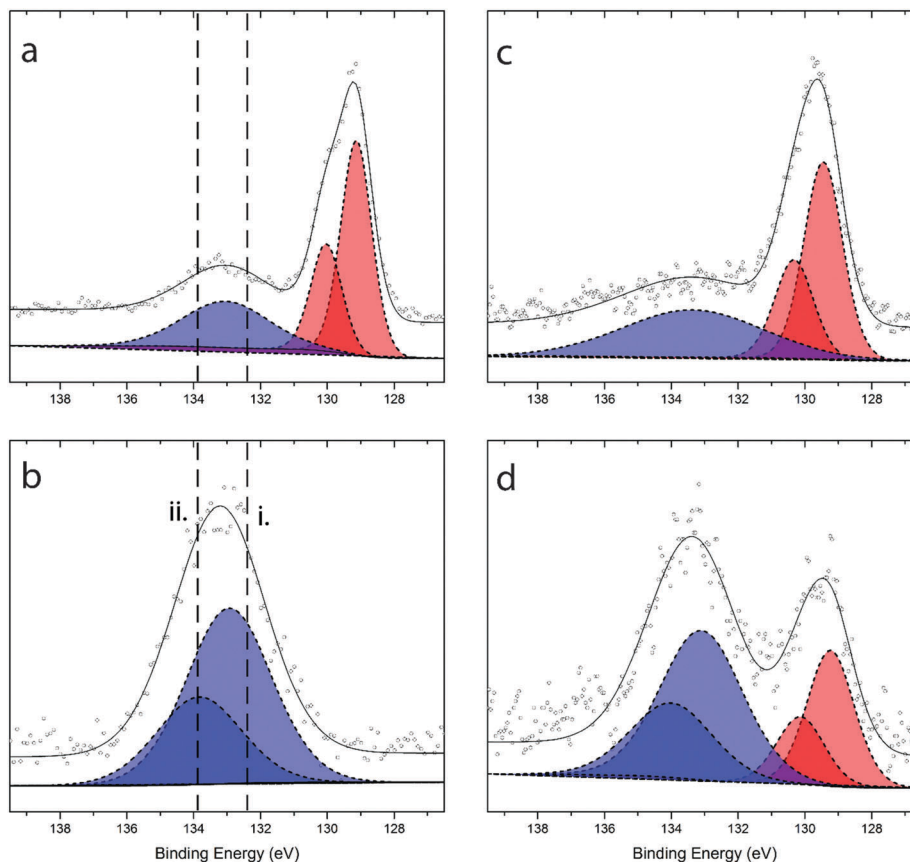


Fig. 3 XPS spectra showing binding energies of P 2p. (a) XPS spectrum of uncorroded  $\text{Fe}_2\text{NiP}$ . (b) The  $\text{Fe}_2\text{NiP}$  sample was corroded in saltwater under anoxic conditions for 48 hours at  $40^\circ\text{C}$ . (c) XPS spectrum of uncorroded  $\text{Fe}_3\text{P}$ . (d)  $\text{Fe}_3\text{P}$  subject to corrosion by de-ionized water at  $80^\circ\text{C}$  for 48 hours. Line i marks the peak position characteristic of potassium hypophosphite and line ii the monobasic potassium phosphate salt.

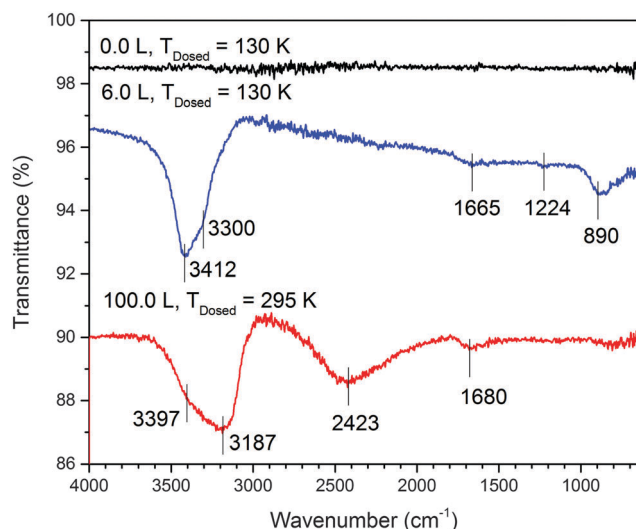


Fig. 4 RAIRS spectra of  $\text{Fe}_2\text{NiP}$  before (black spectrum) and after (blue and red spectra) exposure to  $\text{H}_2\text{O}$ . All spectra were obtained at a surface temperature of  $\leq 130\text{ K}$ . However, the surface temperature was held to  $T_{\text{Dosed}}$  while being exposed to room temperature water.

with  $\text{P}=\text{O}$  stretching frequencies and  $\text{P}-\text{O}-\text{H}$  bending modes on surfaces,<sup>33–36</sup> suggesting oxidation of the schreibersite surface.

Isotopic analysis with  $^{18}\text{O}$  labeled water were also performed and did not show a shift in this frequency. This indicates a chemical interaction between water and schreibersite, even at very low temperatures and pressures.

The experiment with  $T_{\text{Dosed}} = 295\text{ K}$  (red spectrum) required a higher dosage than the experiment with  $T_{\text{Dosed}} = 130\text{ K}$  (blue spectrum) because the sticking coefficient of water in vacuum is lower at the higher surface temperature. For  $T_{\text{Dosed}} = 295\text{ K}$  (red spectrum), the peak at  $3187\text{ cm}^{-1}$  indicates dissociative chemisorption of water into hydroxyls.<sup>37,38</sup> The peak at  $2423\text{ cm}^{-1}$  could be a  $\text{P}-\text{O}-\text{H}$  or a  $\text{P}-\text{H}$  stretch, indicating an interaction of phosphorus with water on the surface of schreibersite.<sup>33–37</sup> Additionally, control experiments of water dosed onto an  $\text{FeNi}$  sample at  $295\text{ K}$  did not show this feature at  $2400\text{ cm}^{-1}$ . Both the features at  $3187$  and  $2423\text{ cm}^{-1}$  suggest a strong chemical interaction between water vapor and schreibersite. The shoulder at  $\sim 3400\text{ cm}^{-1}$  and the relatively weak feature at  $1680\text{ cm}^{-1}$  are indicative of molecular water bound to the surface (*i.e.*, a hydrogen bonded  $\text{O}-\text{H}$  stretch and a  $\text{H}-\text{O}-\text{H}$  scissors motion, respectively).<sup>32,39,40</sup> The difference in features observed for water dosed at low temperature *versus* high temperature, in particular the appearance of peaks corresponding to dissociation of water, suggests that the surface temperature of the mineral is an important aspect of its reactivity.

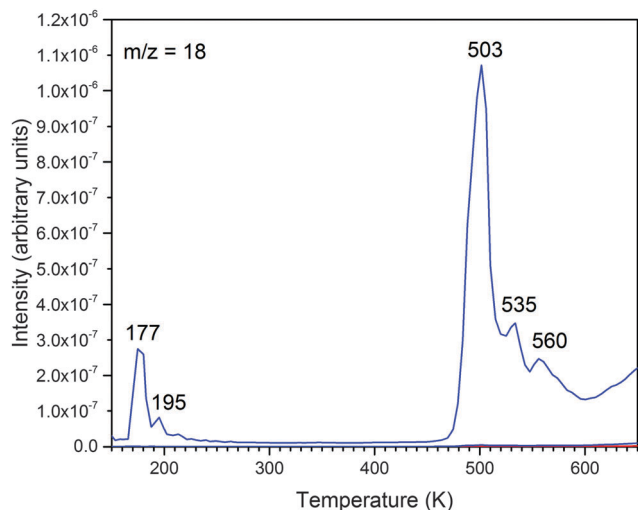


Fig. 5 TPD spectrum after 6 Langmuirs ( $1 \times 10^{-6}$  Torr) of water exposure on a schreibersite ( $\text{Fe}_2\text{NiP}$ ) surface. A ramp rate of  $0.2 \text{ K s}^{-1}$  was used for this experiment.

The TPD spectra shown in Fig. 5 provide further evidence of strong chemical interactions in addition to weaker intermolecular forces between schreibersite and water. In this experiment, 6 Langmuirs of water was dosed onto a 130 K  $\text{Fe}_2\text{NiP}$  surface and the temperature was increased with a ramp rate of  $0.2 \text{ K s}^{-1}$ . Low temperature peaks (*i.e.*, 177 and 195 K) correspond to physisorption of molecular water, while peaks at 503, 535 and 560 K are indicative of hydroxyl groups recombining to form water and desorb after dissociative chemisorption on the surface.  $\text{PO}_x$  species are likely to form anions rather than cations and are not likely to be volatile under the conditions of these experiments. No  $m/z$  peaks corresponding to  $\text{PO}_x^+$  were observed in the TPD spectra. A small signal of  $m/z = 34$  was observed in the TPD, which may be attributable to  $\text{PH}_3$ , or alternatively,  $\text{H}_2\text{O}_2$ .

### 3.4 Corrosion

The corrosion of schreibersite resulted in notable changes to both the schreibersite and the solution it was corroded in. As corrosion progressed, the color of the solutions changed from colorless to what appeared to be a suspension of rust colored precipitate in a clear solution. The corrosion done in sulfidic water resulted in the formation of a dark green solution about a day after corrosion commenced from the initial pale yellow solution. Once exposed to the atmosphere, this color of this solution changed to that observed in the other solutions, *i.e.*, a suspension of rust colored precipitate in a clear solution. Most of the rust colored particulate matter was observed in the seawater corrosion experiments, and the least amount was observed in the deionized water corrosion experiments. After filtering, some of the solutions exhibited a pale blue color.

**P-31 NMR spectroscopy.** The NMR spectra of the corrosion solutions of the samples analyzed indicate the presence of phosphite, orthophosphate, pyrophosphate and hypophosphate. The chemical shifts obtained in doubly deionized water under aerobic conditions were approximately 4.15 ppm, 4.62 ppm,  $-4.07$  ppm and

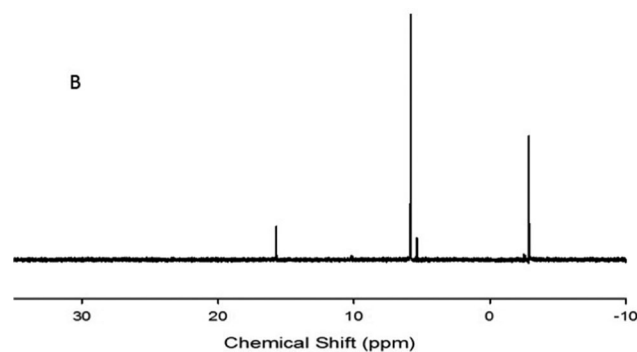


Fig. 6 NMR spectrum of  $\text{Fe}_3\text{P}$  in deionized water. Peaks are identified based on comparison to known standards and H–P coupling constants (*e.g.*, Pasek *et al.* 2007). Note the scale in ppm covers from  $-10$  to  $+35$ , with 0 ppm set as 85%  $\text{H}_3\text{PO}_4$ . From left to right these peaks are hypophosphate ( $\text{P}_2\text{O}_6^{4-}$ ), orthophosphate ( $\text{PO}_4^{3-}$ ), phosphite ( $\text{HPO}_3^{2-}$ ), and pyrophosphate ( $\text{P}_2\text{O}_7^{4-}$ ).

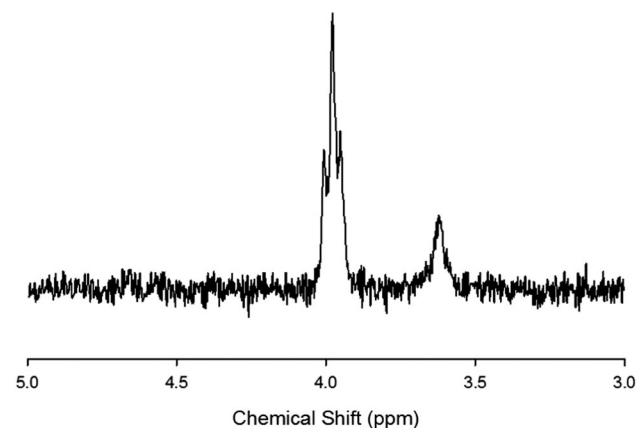


Fig. 7 NMR spectrum indicating the formation of phosphocholine. The ppm scale is referenced to 0, being 85%  $\text{H}_3\text{PO}_4$ . The yield of phosphorylated product within this system is about 12% of the total dissolved P. Such a yield is higher than the yield from reactions in just water of schreibersite<sup>22</sup> but lower than directed reactions with condensed phosphates.<sup>9</sup>

14.5 ppm for phosphite, orthophosphate, pyrophosphate and hypophosphate, respectively (Fig. 6). These peaks correspond to those presented previously for  $\text{Fe}_3\text{P}$  corrosion.<sup>10</sup>

**Phosphorylation of choline.** The NMR analysis of the solution obtained after the phosphorylation experiment indicated the presence of phosphocholine based on the presence of the triplet at chemical shift of approximately 3.9 ppm (Fig. 7). The  $J$ -coupling of this triplet is about 7.5 Hz, indicative of a 3-bond P–H interaction, as in  $\text{CH}_2\text{--O--P}$ . The  $\sim 4$  ppm region of a  $^{31}\text{P}$  NMR spectrum is characteristic of orthophosphate monoesters, and, for these reasons, the triplet is assigned to phosphocholine.

## 4. Discussion

### 4.1 Synthesis

Schreibersite can be synthesized by mixing stoichiometric ratios of elemental iron, nickel, and phosphorus and heating for the aforementioned time. Further, characterization of the

mineral using XRD, microprobe, Raman,<sup>15</sup> and XPS all demonstrate strong similarity between this material and meteoritic schreibersite, with respect to crystal structure, composition, and redox state of elements. The densest schreibersite was made when the product was heated to the melting point after 235 hours. These samples polished easily. While the appearance of these samples were different from others synthesized without heating to the melting point afterwards, the characterization analyses indicated that both types of samples were schreibersite.

#### 4.2 Surface oxidation characterization

The oxidation state of P, Fe, and Ni on the surface of the synthetic schreibersite is most consistent with metallic bonding (Fig. 3). A thin layer of oxide may also be present on the surface, though this can be removed with sputtering to reveal material with a more elemental nature. However, this surface is rather reactive, as shown by Fig. 4 and 5.

Schreibersite is quite reactive toward water. When placed under vacuum at low temperature, water spontaneously sticks to and reacts with the schreibersite surface to generate new bonds involving P, as well as dissociating upon contact with the surface. These results demonstrate that schreibersite is quite reactive even under low temperatures and with water, a relatively weak oxidant. To this end, effectively all schreibersite placed in wet environments will have an oxidized surface. Therefore, the surface of schreibersite on the Hadean earth will have been oxidized, even if the atmosphere as a whole was reducing; hence, surficial oxidation and phosphorylation by schreibersite in a reducing environment remains plausible.

#### 4.3 Corrosion

During corrosion experiments there were color changes from green to brown, which suggest the oxidation of  $\text{Fe}^{2+}$  to  $\text{Fe}^{3+}$  and the binding energies obtained from the XPS analyses of the corroded  $\text{Fe}_2\text{NiP}$  and  $\text{Fe}_3\text{P}$  samples indicated that the P on the surface was indeed oxidized. Some of the solutions had a light blue color suggesting the presence of oxidized Ni. The solution chemistry, therefore, confirms the surface chemistry.

The NMR spectra of the filtered solutions after corrosion experiments provide further evidence that this synthetic method produces a useful proxy for natural schreibersite. Corrosion of our prepared samples replicate prior work on corrosion of both natural schreibersite and  $\text{Fe}_3\text{P}$ .<sup>10,11,41</sup> The chemical shifts in our spectra agree with those demonstrated in the aforementioned papers.

The synthesized schreibersite has now been demonstrated to phosphorylate choline, making phosphocholine. Synthesis of this molecule demonstrates that schreibersite would react with organic compounds to generate prebiotic molecules. This reaction occurred within a deep eutectic mixture, the first that has employed schreibersite as a P source.<sup>42</sup> The phosphate ester of choline can also be formed when struvite is used as a P source but the prebiotic relevance of struvite is questionable.<sup>43</sup>

## 5. Conclusions

This work demonstrates the successful synthesis of schreibersite, and that this synthetic schreibersite is a useful analogue for meteoritic schreibersite. Unlike commercially available  $\text{Fe}_3\text{P}$ , it contains nickel and hence is compositionally closer to natural schreibersite. It is also easier and less expensive to produce this synthetic schreibersite than it is to purchase and extract meteoritic schreibersite making it ideal for studies requiring schreibersite as a reactant. These samples are structurally, compositionally, and electronically identical to meteoritic schreibersite, and produce similar chemical compounds when reacted with water at room temperature.

Additionally, the oxidation of the surface of schreibersite appears inevitable in any wet environment. Schreibersite is an effective reducing agent, releasing hydrogen from water, and binding hydroxyls to the surface, as well as forming P–O bonds. This implies that a schreibersite on a meteoroid surface that is heated with water under low pressure ( $\sim$ within the vacuum of space) will still have an oxidized surface. To this end, a meteorite that falls on a wet planet will still bear a reactive P-oxide surface after a relatively short time period, independent of the composition of the atmosphere.

The corrosion products of this synthetic schreibersite are identical to those of synthetic  $\text{Fe}_3\text{P}$ ,<sup>10</sup> and to meteoritic schreibersite,<sup>24</sup> and thus this material verifies prior experiments with  $\text{Fe}_3\text{P}$  as being valid as a schreibersite analogue. The presence of nickel does not significantly change the corrosion process of schreibersite. Surface studies of these minerals also show that the surface is characterized by an oxidized material, with an oxidation state between +1 and +5, requiring significant electron transport from the initial oxidation state of  $-1$ . This result, while not terribly surprising given that prior studies have demonstrated similar phenomena for meteoritic schreibersite, does serve to confirm chemical similarity between the synthesized material and meteoritic schreibersite.

Finally, this is the first full report of the nickel-bearing variety synthetic analogue of schreibersite that has been shown to form organophosphates by reaction in water, followed by reaction within a deep eutectic solvent. Deep eutectic solvents arise spontaneously by evaporation of water, and hence these may be formed merely by the drying down of solutions on minerals. Formation of organophosphates, long thought difficult, is relatively facile under these conditions. A potentially prebiotic environment where such a chemical reaction would be relevant would be a shallow pool that experiences periods of drying. A thin layer of organic eutectics would result, with a low water activity that promotes phosphorylation. Phosphorylation by schreibersite now has been demonstrated with glycerol, nucleosides, and with choline, suggesting that schreibersite is a fairly robust phosphorylation source.<sup>21,22</sup>

## Acknowledgements

This work was jointly supported by NSF and the NASA Astrobiology program under the NSF Center for Chemical Evolution, CHE-1504217. M. A. P. was also supported by the NASA Exobiology



and Evolutionary Biology program, grant NNX14AN96G. We thank Edwin Rivera from the USF NMR facility for research assistance.

## References

- 1 F. H. Westheimer, *Science*, 1987, **235**(4793), 1173–1178.
- 2 E. Maciá, M. V. Hernández and J. Oró, *Origins Life Evol. Biospheres*, 1997, **27**(5–6), 459–480.
- 3 C. Ponnampertuma and R. Mack, *Science*, 1965, **148**(36), 1221–1223.
- 4 Y. Yamagata, T. Matsukawa, T. Mohri and K. Inomata, *Nature*, 1979, **282**(5736), 284–286.
- 5 R. Krishnamurthy, G. Arrhenius and A. Eschenmoser, *Origins Life Evol. Biospheres*, 1999, **29**(4), 333–354.
- 6 G. Costanzo, R. Saladino, C. Crestini, F. Ciciriello and E. Di Mauro, *J. Biol. Chem.*, 2007, **282**(23), 16729–16735.
- 7 T. Lönnberg, *Beilstein J. Org. Chem.*, 2016, **12**(1), 670–673.
- 8 A. Lazcano and S. L. Miller, *Cell*, 1996, **85**(6), 793–798.
- 9 M. A. Pasek and T. P. Kee, *Origins of Life: The Primal Self-Organization*, Springer, Berlin Heidelberg, 2011, pp. 57–84.
- 10 M. A. Pasek and D. S. Lauretta, *Astrobiology*, 2005, **5**(4), 515–535.
- 11 D. E. Bryant and T. P. Kee, *Chem. Commun.*, 2006, 2344–2346.
- 12 A. Gulick, *Am. Sci.*, 1955, 479–489.
- 13 M. Pelavin, D. N. Hendrickson, J. M. Hollander and W. L. Jolly, *J. Phys. Chem.*, 1970, **74**(5), 1116–1121.
- 14 D. E. Bryant, D. Greenfield, D. Walshaw, R. D. Johnson, B. R. Herschy, C. Smith, M. A. Pasek, R. Telford, I. Scowen, T. Munshi and H. G. Edwards, *Geochim. Cosmochim. Acta*, 2013, **109**, 90–112.
- 15 C. Pirim, M. A. Pasek, D. A. Sokolov, A. N. Sidorov, R. D. Gann and T. M. Orlando, *Geochim. Cosmochim. Acta*, 2014, **140**, 259–274.
- 16 S. N. Britvin, M. N. Murashko, Y. Vapnik, Y. S. Polekhovsky and S. V. Krivovichev, *Sci. Rep.*, 2015, **5**, 8355.
- 17 E. J. Essene and D. C. Fisher, *Science*, 1986, **234**(4773), 189–193.
- 18 M. A. Pasek, K. Block and V. Pasek, *Contrib. Mineral. Petrol.*, 2012, **164**(3), 477–492.
- 19 M. A. Pasek, B. Herschy and T. P. Kee, *Origins Life Evol. Biospheres*, 2015, **45**(1), 207–218.
- 20 S. Marchi, W. F. Bottke, L. T. Elkins-Tanton, M. Bierhaus, K. Wuennemann, A. Morbidelli and D. A. Kring, *Nature*, 2014, **511**(7511), 578–582.
- 21 M. A. Pasek, J. P. Harnmeijer, R. Buick, M. Gull and Z. Atlas, *Proc. Natl. Acad. Sci. U. S. A.*, 2013, **110**(25), 10089–10094.
- 22 M. Gull, M. A. Mojica, F. M. Fernandez, D. A. Gaul, T. M. Orlando, C. L. Liotta and M. A. Pasek, *Sci. Rep.*, 2015, **5**, 17198.
- 23 M. A. Pasek, T. P. Kee, D. E. Bryant, A. A. Pavlov and J. I. Lunine, *Angew. Chem., Int. Ed.*, 2008, **47**(41), 7918–7920.
- 24 D. E. Bryant, D. Greenfield, R. D. Walshaw, S. M. Evans, A. E. Nimmo, C. L. Smith, L. Wang, M. A. Pasek and T. P. Kee, *Int. J. Astrobiol.*, 2009, **8**(01), 27–36.
- 25 B. Rasmussen and R. Buick, *Geology*, 1999, **27**(2), 115–118.
- 26 L. R. Kump, *Nature*, 2008, **451**(7176), 277–278.
- 27 R. Skála and M. Drábek, *Powder Diffr.*, 2002, **17**(04), 322–325.
- 28 M. Gull, M. Zhou, F. M. Fernández and M. A. Pasek, *J. Mol. Evol.*, 2014, **78**(2), 109–117.
- 29 A. S. Bolina, A. J. Wolff and W. A. Brown, *J. Phys. Chem. B*, 2005, **109**, 16836–16845.
- 30 A. Baro and W. Erley, *J. Vac. Sci. Technol.*, 1982, **20**, 580–583.
- 31 W. Hung, J. Schwartz and S. L. Bernasek, *Surf. Sci.*, 1991, **248**, 332–342.
- 32 W. Hung, J. Schwartz and S. Bernasek, *Surf. Sci.*, 1993, **294**, 21–32.
- 33 P. Connor and A. J. McQuillan, *Langmuir*, 1999, **15**, 2916–2921.
- 34 T. Bezrodna, G. Puchkovska, V. Shymanovska, J. Baran and H. Ratajczak, *J. Mol. Struct.*, 2004, **700**, 175–181.
- 35 R. Carter, C. Gierczak and R. Dickie, *Appl. Spectrosc.*, 1986, **40**, 649–655.
- 36 C. Dayanand, G. Bhikshamaiah, V. J. Tyagaraju, M. Salagram and A. K. Murthy, *J. Mater. Sci.*, 1996, **31**, 1945–1967.
- 37 S. Koutsopoulos, *J. Biomed. Mater. Res.*, 2002, **62**, 600–612.
- 38 E. E. Berry and C. B. Baddiel, *Spectrochim. Acta, Part A*, 1967, **23**, 1781–1792.
- 39 A. M. Turner, M. J. Abplanalp, S. Y. Chen, Y. T. Chen, A. H. Chang and R. I. Kaiser, *Phys. Chem. Chem. Phys.*, 2015, **17**, 27281–27291.
- 40 M. Hock, U. Seip, I. Bassignana, K. Wagemann and J. Küppers, *Surf. Sci. Lett.*, 1986, **177**, L978–L982.
- 41 M. A. Pasek, J. P. Dworkin and D. S. Lauretta, *Geochim. Cosmochim. Acta*, 2007, **71**(7), 1721–1736.
- 42 A. P. Abbott, D. Boothby, G. Capper, D. L. Davies and R. K. Rasheed, *J. Am. Chem. Soc.*, 2004, **126**(29), 9142–9147.
- 43 M. Gull and M. A. Pasek, *Life*, 2013, **3**(2), 321–330.